

Three-level laser heat engine at optimal performance with ecological function

Varinder Singh* and Ramandeep S. Johal†

*Department of Physical Sciences,
Indian Institute of Science Education and Research Mohali,
Sector 81, S.A.S. Nagar,
Manauli PO 140306, Punjab, India*

Although classical and quantum heat engines work on entirely different fundamental principles, there is an underlying similarity. For instance, the form of efficiency at optimal performance may be similar for both types of engines. In this work, we study a three-level laser quantum heat engine operating at maximum ecological function (EF) which represents a compromise between the power output and the loss of power due to entropy production. We derive analytic expressions for efficiency under the assumptions of strong matter-field coupling and high bath temperatures. Upper and lower bounds on the efficiency exist in case of extreme asymmetric dissipation when the ratio of system-bath coupling constants at the hot and the cold contacts respectively approaches, zero or infinity. These bounds have been established previously for various classical models of Carnot-like engines. We conclude that while the engine produces at least 75% of the power output as compared with the maximum power conditions, the fractional loss of power is appreciably low in case of the engine operating at maximum EF, thus making this objective function relevant from an environmental point of view.

I. INTRODUCTION

With the explosion of interest in quantum thermodynamics [1–3], we may be entering an era whereby energy conversion devices are able to harness non-classical properties like coherence between internal states, entanglement, quantum degeneracy and so on. Thus, it is of great importance to ascertain the extent up to which these devices may surpass the performance of macroscopic, classical heat devices.

On the other hand, rising concerns about the effects of human activity on the environment make it prudent that the new technologies be better from an ecological point of view. Most comparisons that are usually studied between quantum [4–17] and classical models of heat engines [18–20], focus on the optimization of power output [19, 21–29]. However, to be ecologically aware, we must care about the extent of entropy production which ultimately impacts the environment. As has been noted [30, 31], real thermal plants and practical heat engines may not operate at maximum power point, but rather in a regime with a slightly smaller power output and appreciably larger efficiency. In recent years, a few such alternate measures of performance have been studied. Thus, the ecological function [32, 33] or Omega function [34] and efficient-power function [35, 36] fall under such a category, as they pay equal attention to both power and efficiency.

In this work, we study the optimization of ecological function in the performance of a three-level steady state laser heat engine [37]. The ecological function (EF) is

defined as [32]

$$E = P - T_c \dot{S}_{\text{tot}}, \quad (1)$$

where P is the power output, T_c is the temperature of the cold reservoir and \dot{S}_{tot} is the total rate of entropy production. Optimization of EF represents a compromise between the power output and the loss of power due to entropy production. In the context of classical models, this function suggests optimal working conditions which lead to a drop of about 20% in power output (compared to maximum power output), but on the other hand, reduce the entropy production by about 70% [32].

Our second motivation for this analysis is to study the correspondence between classical and quantum heat engines (QHEs). In most of the studies so far, QHEs show exotic behavior owing to additional resources such as quantum coherence [15, 29, 38–43], quantum entanglement [44–48], squeezed baths [49–51], among others. Otherwise, QHEs may show a remarkable similarity to macroscopic heat engines. In such cases, Carnot efficiency provides an upper bound on the efficiencies of QHEs operating between two heat reservoirs. The irreversible operation of quantum engines with finite power output has many similarities to macroscopic endoreversible engines and the low-dissipation model [19, 21]. Also in the high temperatures limit, QHEs are expected to behave like classical heat engines [52, 53]. We confirm these expectations in the analysis of the three-level laser engine using the ecological function.

The paper is organised as follows. In Sec.II, we discuss the model of three-level laser quantum heat engine. In Sec. III, we obtain the general expression for the efficiency of the engine operating at maximum EF and find lower and upper bounds on the efficiency for two different optimization schemes. In Secs. IV and V, we compare the performance of heat engine operating at maximum

* varindersingh@iisermohali.ac.in

† rsjohal@iisermohali.ac.in

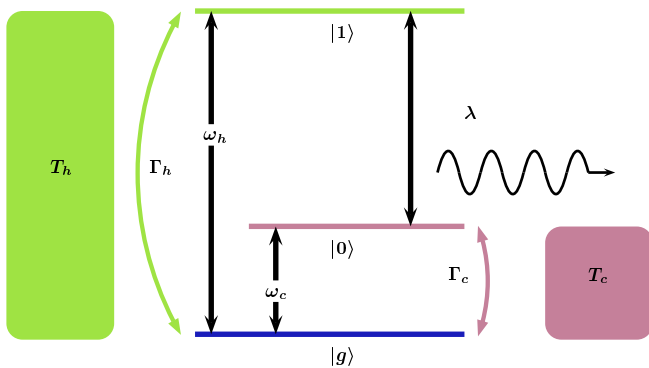


FIG. 1. (Color online) Model of three-level laser heat engine continuously coupled to two reservoirs of temperatures T_h and T_c having coupling constants Γ_h and Γ_c , respectively. The system is interacting with a classical single mode field. λ represents the strength of matter-field coupling.

EF to the engine operating at maximum power. We conclude in Sec. VI by highlighting the key results.

II. MODEL OF THREE-LEVEL LASER QUANTUM HEAT ENGINE

One of the simplest QHEs is three-level laser heat engine [37] introduced by Scovil and Schulz-Dubois (SSD). It converts the incoherent thermal energy of heat reservoirs into a coherent laser output. The model has been studied extensively in the literature, and three-level systems are also employed to study quantum absorption refrigerators [54–57]. The model proposed by Scovil and DuBois was further analyzed by Geva and Kosloff [58, 59] in the spirit of finite time thermodynamics. In the presence of strong time dependent external fields, they optimized the power output of the amplifier w.r.t different control parameters. In their model, the second law of thermodynamics is generally satisfied if one incorporates the effect of external field on the dissipative superoperator. In a series of papers [60–62], Boukobza and Tannor formulated a new way to partition energy into heat and work [63]. They applied their analysis to a three level amplifier continuously coupled to two reservoirs and to a classical single mode field [62]. Their formulation is quite general and one does not need to incorporate the effect of external field on the dissipative term of the Liouvillian, and yet the second law of thermodynamics is always satisfied at the steady state. In this paper, we use the formalism of Ref. [62] to study the optimal performance of a three-level QHE operating in high temperature regime.

More precisely, the model consists of a three-level system continuously coupled to two thermal reservoirs and to a single mode classical field (see Fig. 1). A hot reservoir at temperature T_h drives the transition between the ground level $|g\rangle$ and top level $|1\rangle$, whereas the transition between the intermediate level $|0\rangle$ and ground level

$|g\rangle$ is constantly de-excited by a cold reservoir at temperature T_c . The power output mechanism is modeled by coupling the levels $|0\rangle$ and $|1\rangle$ to a classical single mode field. The Hamiltonian of the system is given by: $H_0 = \hbar \sum \omega_k |k\rangle \langle k|$ where the summation runs over all three states and ω_k represents the relevant atomic frequency. The interaction with the single mode lasing field of frequency ω , under the rotating wave approximation, is described by the semiclassical hamiltonian: $V(t) = \hbar \lambda (e^{i\omega t} |1\rangle \langle 0| + e^{-i\omega t} |0\rangle \langle 1|)$; λ is the matter-field coupling constant. The time evolution of the system is described by the following master equation:

$$\dot{\rho} = -\frac{i}{\hbar} [H_0 + V(t), \rho] + \mathcal{L}_h[\rho] + \mathcal{L}_c[\rho], \quad (2)$$

where $\mathcal{L}_{h(c)}$ represents the dissipative Lindblad superoperator describing the system-bath interaction with the hot (cold) reservoir:

$$\begin{aligned} \mathcal{L}_h[\rho] = & \Gamma_h (n_h + 1) (2|g\rangle \langle g| \rho_{11} - |1\rangle \langle 1| \rho - \rho |1\rangle \langle 1|) \\ & + \Gamma_h n_h (2|1\rangle \langle 1| \rho_{gg} - |g\rangle \langle g| \rho - \rho |g\rangle \langle g|), \end{aligned} \quad (3)$$

$$\begin{aligned} \mathcal{L}_c[\rho] = & \Gamma_c (n_c + 1) (2|g\rangle \langle g| \rho_{00} - |0\rangle \langle 0| \rho - \rho |0\rangle \langle 0|) \\ & + \Gamma_c n_c (2|0\rangle \langle 0| \rho_{gg} - |g\rangle \langle g| \rho - \rho |g\rangle \langle g|). \end{aligned} \quad (4)$$

Here Γ_h and Γ_c are the Weisskopf-Wigner decay constants, and $n_{h(c)} = 1/(\exp[\hbar\omega_{h(c)}/k_B T_{h(c)}] - 1)$ is average occupation number of photons in hot (cold) reservoir satisfying the relations $\omega_c = \omega_0 - \omega_g$, $\omega_h = \omega_1 - \omega_g$.

In this model, it is possible to find a rotating frame in which the steady-state density matrix ρ_R is time independent [62]. Defining $\bar{H} = \hbar(\omega_g |g\rangle \langle g| + \frac{\omega}{2} |1\rangle \langle 1| - \frac{\omega}{2} |0\rangle \langle 0|)$, an arbitrary operator A in the rotating frame is given by $A_R = e^{i\bar{H}t/\hbar} A e^{-i\bar{H}t/\hbar}$. It can be seen that $\mathcal{L}_h[\rho]$ and $\mathcal{L}_c[\rho]$ remain unchanged under this transformation. Time evolution of the system density matrix in the rotating frame can be written as

$$\dot{\rho}_R = -\frac{i}{\hbar} [H_0 - \bar{H} + V_R, \rho_R] + \mathcal{L}_h[\rho_R] + \mathcal{L}_c[\rho_R] \quad (5)$$

where $V_R = \hbar \lambda (|1\rangle \langle 0| + |0\rangle \langle 1|)$.

For a weak system-bath coupling, the output power, the heat flux and the efficiency of the engine can be defined [62], as follows:

$$P = \frac{i}{\hbar} \text{Tr}([H_0, V_R] \rho_R), \quad (6)$$

$$\dot{Q}_h = \text{Tr}(\mathcal{L}_h[\rho_R] H_0), \quad (7)$$

$$\eta = \frac{P}{\dot{Q}_h}. \quad (8)$$

Plugging the expressions for H_0 , V_R and $\mathcal{L}_h[\rho_R]$, and calculating the traces (see Appendix A) appearing on the right hand side of Eqs. (6) and (7), the power and heat flux can be written as:

$$P = i\hbar \lambda (\omega_h - \omega_c) (\rho_{01} - \rho_{10}), \quad (9)$$

$$\dot{Q}_h = i\hbar \lambda \omega_h (\rho_{01} - \rho_{10}), \quad (10)$$

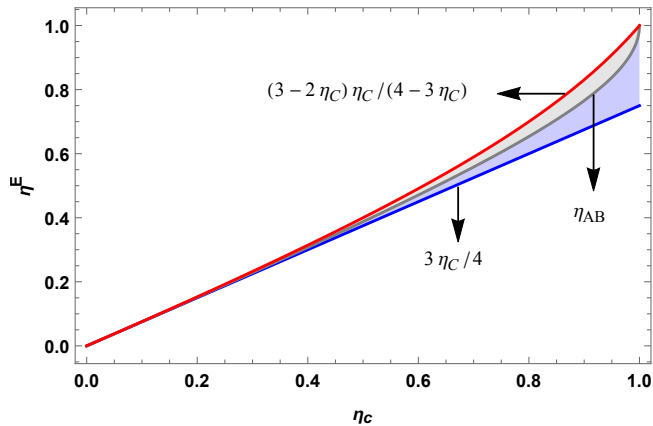


FIG. 2. (Color online) Efficiency η^E versus the Carnot efficiency η_C for the SSD engine. η_{AB} serves as the upper bound for the case with fixed ω_h and the lower bound for a fixed ω_c .

where $\rho_{01} = \langle 0|\rho_R|1\rangle$ and $\rho_{10} = \langle 1|\rho_R|0\rangle$. Then, the efficiency is given by

$$\eta = 1 - \frac{\omega_c}{\omega_h}. \quad (11)$$

From Eq.(B3), the positive power production condition implies that $\omega_c/\omega_h \geq T_c/T_h$. Hence $\eta \leq \eta_C$.

III. OPTIMIZATION OF ECOLOGICAL FUNCTION

The optimal performance of SSD engine at maximum power has already been studied recently [29]. In this work, we optimize the EF which represents a trade-off between power output and loss of power in the system. We identify the total rate of entropy production in the heat reservoirs due to operation of our engine as

$$\dot{S}_{\text{tot}} = \frac{\dot{Q}_c}{T_c} - \frac{\dot{Q}_h}{T_h}. \quad (12)$$

In the steady state, the entropy of the system remains constant. Substituting Eq. (12) in (1), the EF can be written as

$$E = 2P - (1 - \tau)\dot{Q}_h, \quad (13)$$

where $\tau = T_c/T_h$. Using Eqs. (9) and (10), we recast Eq. (13) as

$$E = i\hbar\lambda(\rho_{01} - \rho_{10})[2(\omega_h - \omega_c) - (1 - \tau)\omega_h]. \quad (14)$$

Now we optimize E w.r.t. the transition frequencies ω_h and ω_c , and then calculate the corresponding efficiency at maximum ecological function (EMEF). In order to obtain analytic expressions in a closed form for the EMEF, we will work in the high temperatures regime and assume the matter-field coupling to be very strong as compared to the system-bath coupling ($\lambda \gg \Gamma_{h,c}$). In the high temperatures limit, we set $n_h \simeq k_B T_h / \hbar \omega_h$ and $n_c \simeq k_B T_c / \hbar \omega_c$. The function E can then be written in the following form (Appendix B)

$$E \simeq \frac{2\hbar\Gamma_h(\omega_c - \tau\omega_h)[2(\omega_h - \omega_c) - (1 - \tau)\omega_h]}{3(\omega_c\gamma + \tau\omega_h)}, \quad (15)$$

where $\gamma = \Gamma_h/\Gamma_c$. Here, we choose frequencies ω_h and ω_c as control parameters. Note that it is not possible to optimize E in Eq. (15) w.r.t both ω_c and ω_h simultaneously. Such two-parameter optimization yields the trivial solution, $\omega_c = \omega_h = 0$. Therefore, we will consider the optimization problem w.r.t one parameter only, while keeping the other one fixed at some given value. First, keeping ω_h fixed, we optimize Eq. (15) w.r.t. ω_c , i.e., by setting $\partial E/\partial\omega_c = 0$, we evaluate EMEF as

$$\eta_{\omega_h}^E = 1 + \frac{\tau}{\gamma} - \frac{\sqrt{(1 + \gamma)\tau[\gamma + (2 + \gamma)\tau]}}{\sqrt{2}\gamma}, \quad (16)$$

Now, $\eta_{\omega_h}^E$ is a monotonically increasing function of γ . Therefore, we can obtain the lower and upper bounds of EMEF by letting $\gamma \rightarrow 0$ and $\gamma \rightarrow \infty$, respectively. Further, writing in terms of $\eta_C = 1 - \tau$, we have

$$\frac{3}{4}\eta_C \leq \eta_{\omega_h}^E \leq 1 - \sqrt{\frac{(1 - \eta_C)(2 - \eta_C)}{2}}. \quad (17)$$

The lower bound, $3\eta_C/4$, obtained here is also derived as the lower bound for low-dissipation heat engines [64] and minimally nonlinear irreversible heat engines [65]. The upper bound, $\sqrt{(1 - \eta_C)(2 - \eta_C)}/2$, was first derived by Angulo-Brown for a classical endoreversible heat engine [32]. Henceforth, we denote it as η_{AB} . Under the conditions of tight-coupling and symmetric dissipation, η_{AB} can also be obtained for low-dissipation heat engines [64] and minimally nonlinear irreversible heat engines [65].

Alternately, we may fix the value of ω_c and optimize E w.r.t ω_h , thus obtaining EMEF in the following form

$$\eta_{\omega_c}^E = \frac{\gamma(1 - \tau^2) + 2(1 + \gamma)\tau - \sqrt{(1 + \gamma)\tau^2(1 + \tau)[\gamma + (2 + \gamma)\tau]}}{\gamma + 2\tau + 3\gamma\tau}. \quad (18)$$

Again $\eta_{\omega_c}^E$ is monotonic increasing function of γ . So we obtain lower and upper bounds on EMEF in the limiting cases $\gamma \rightarrow 0$ and $\gamma \rightarrow \infty$, respectively. In terms of η_C , we have

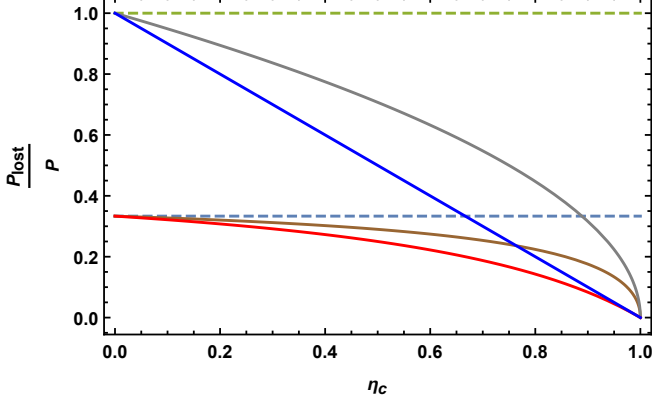


FIG. 3. (Color online) Comparison of the ratios of power lost to power output, versus $\eta_C = 1 - \tau$, for the optimization of two different target functions - Ecological function and power output. The low lying set of curves [Eqs. (21) and (22)] represent the case of optimal EF, whereas the upper curves [Eqs. (23) and (24)] represent the case of optimal power output.

$$\eta_{AB} \leq \eta_{\omega_c}^E \leq \frac{3 - 2\eta_C}{4 - 3\eta_C} \eta_C. \quad (19)$$

Under the conditions of extreme dissipation, upper bound $(3 - 2\eta_C)\eta_C/(4 - 3\eta_C)$ reported here, also serves as the upper bound for the low-dissipation [19] and minimally non-linear irreversible [65] heat engines.

IV. FRACTIONAL LOSS OF POWER AT MAXIMUM ECOLOGICAL FUNCTION AND MAXIMUM POWER OUTPUT

In this section, we compare performance of the three-level heat engine operating at maximum EF to the engine operating at maximum power. Now, in the definition of EF, $T_c \dot{S}_{\text{tot}} \equiv P_{\text{lost}}$ represents the loss of power. So, we rewrite EF as $E = P - P_{\text{lost}}$ and after rearranging terms, we obtain

$$R' \equiv \frac{P_{\text{lost}}}{P} = 1 - \frac{E}{P} \equiv 1 - R. \quad (20)$$

We calculate R , and hence R' , in four different cases, as discussed in Appendix C. For optimization of EF w.r.t ω_c , at a fixed ω_h , the ratio of optimal EF, $E_{\text{eco}}^{*(\omega_h)}$, to the power at maximum EF, $P_{\text{eco}}^{*(\omega_h)}$, is given by Eq. (C3). We mention here only the limiting cases $\gamma \rightarrow 0$ and $\gamma \rightarrow \infty$, for which the respective equations for R' can be derived using Eqs. (20) and (C4):

$$R'_{\text{eco}(0)}^{\omega_h} = \frac{1}{3}, \quad R'_{\text{eco}(\infty)}^{\omega_h} = \frac{\sqrt{\tau}}{\sqrt{\tau} + \sqrt{2(1+\tau)}}. \quad (21)$$

Similar equations for the optimization of E w.r.t ω_h , while keeping ω_c fixed, are given by

$$R'_{\text{eco}(0)}^{\omega_c} = \frac{\sqrt{\tau}}{\sqrt{\tau} + \sqrt{2(1+\tau)}}, \quad R'_{\text{eco}(\infty)}^{\omega_c} = \frac{\tau}{1+2\tau}. \quad (22)$$

All the above expressions approach the value $1/3$ near equilibrium, i.e. for small temperature differences. The fractional loss of power is, in general, higher for the case with fixed ω_h than with a fixed ω_c . As γ increases, the fractional loss of power decreases. Also note that $R'_{\text{eco}(\infty)}^{\omega_h} = R'_{\text{eco}(0)}^{\omega_c}$, as expected, since efficiencies are also equal for the corresponding cases, $\eta_{\omega_c}^E(\infty) = \eta_{\omega_h}^E(0) = \eta_{AB}$, as can be seen from Eqs. (17) and (19).

Next we calculate the ratio of power loss to power output for the cases when we optimize power output. First, we discuss the case when the optimization is performed over ω_c . As seen from Eq. (C13), $R'_{\text{pow}(0)}^{\omega_h} = 0$, which indicates that corresponding EF is zero in this case, which in turn implies that the loss of power is equal to the power output. The ratios R' for the extreme cases $\gamma \rightarrow 0$ and $\gamma \rightarrow \infty$ are given by

$$R'_{\text{pow}(0)}^{\omega_h} = 1, \quad R'_{\text{pow}(\infty)}^{\omega_h} = \sqrt{\tau} \quad (23)$$

The corresponding expressions, at optimal power output w.r.t ω_h , are given by

$$R'_{\text{pow}(0)}^{\omega_c} = R'_{\text{pow}(\infty)}^{\omega_h}, \quad R'_{\text{pow}(\infty)}^{\omega_c} = \tau. \quad (24)$$

Similar trend is observed for the fractional loss of power in this case also, as noted for the optimal EF above. More importantly, for near equilibrium conditions (small values of η_C), optimal EF yields lower values of fractional loss of power as compared to optimal power output.

V. RATIO OF POWER AT MAXIMUM ECOLOGICAL FUNCTION TO MAXIMUM POWER

Fig. 3 indicates that the fractional loss of power is larger when the three-level laser heat engine operates at maximum power as compared to the engine operating at maximum EF. So, it is useful to evaluate the ratio of power output at maximum EF to the maximum power. Defining $\bar{R}_{\gamma}^{\omega_h} = P_{\text{eco}}^{*(\omega_h)}/P_{\text{pow}}^{*(\omega_h)}$ (see Eqs. (C2) and (C10)), and by taking limits $\gamma \rightarrow 0$ and $\gamma \rightarrow \infty$, we have following two equations, respectively

$$\bar{R}_0^{\omega_h} = \frac{1 + 3\tau - \frac{\tau(3+5\tau)}{\sqrt{1+3\tau}}}{1 + 3\tau - 2\sqrt{2\tau(1+\tau)}}, \quad \bar{R}_{\infty}^{\omega_h} = \frac{1 + \tau - \frac{\tau(3+\tau)}{\sqrt{2\tau(1+\tau)}}}{(1 - \sqrt{\tau})^2} \quad (25)$$

Similar equations can be obtained for fixed ω_c by dividing $P_{\text{eco}}^{*(\omega_c)}$ with $P_{\text{pow}}^{*(\omega_c)}$ (see Eqs. (C6) and (C15)) and repeating the above mentioned step. Thus we have

$$\bar{R}_0^{\omega_c} = \bar{R}_{\infty}^{\omega_h}, \quad \bar{R}_{\infty}^{\omega_c} = \frac{1 + 2\tau}{(1 + \tau)^2}. \quad (26)$$

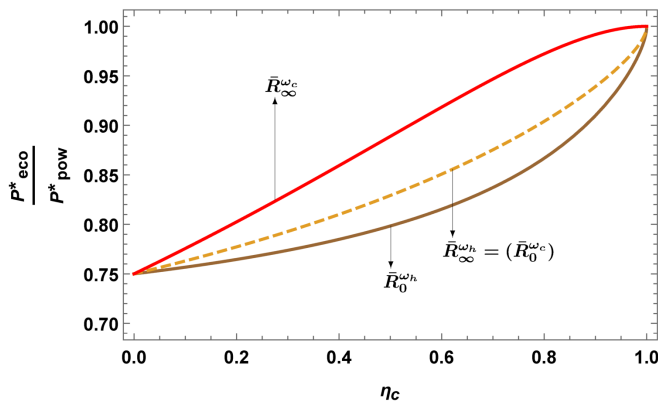


FIG. 4. (Color online) Comparison of the ratio \bar{R} of the power output at maximum EF to the maximum power [Eqs. (25) and (26)].

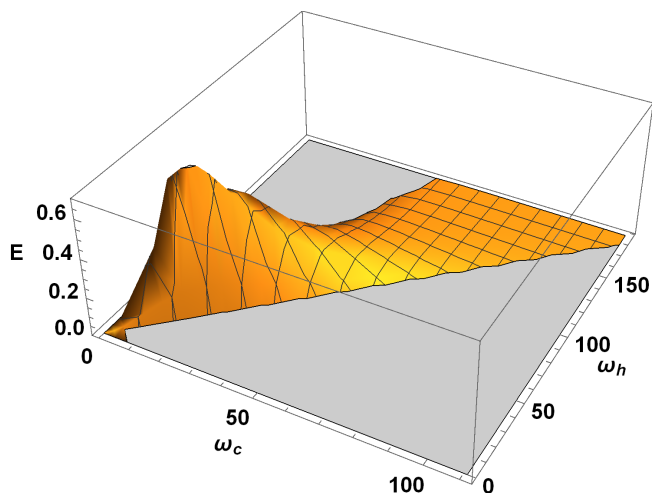


FIG. 5. (Color online) 3D-plot of EF [Eq. (A14)] in terms of control frequencies ω_c and ω_h for $\hbar = 1, k_B = 1, \Gamma_h = \Gamma_c = 1, \lambda = 1, T_h = 20, T_c = 5$.

Again $\bar{R}_{\infty}^{\omega_h}$ is equal to $\bar{R}_0^{\omega_c}$ as expected. Plotting Eqs. (25) and (26) in Fig. 4, we observe that at least 75% of the maximum power is produced in the maximum EF regime. The ratio $P_{\text{eco}}^*/P_{\text{pow}}^*$ increases with increasing η_C , which is expected since the efficiency of the engine also increases, while the dissipation decreases.

VI. CONCLUDING REMARKS

We have analyzed and optimized thermodynamic performance of SSD heat engine with the ecological function (EF). Here we performed one parameter optimization of EF alternatively w.r.t ω_c (ω_h fixed) and ω_h (ω_c fixed) and obtained the general expressions for the EMEF in high temperatures regime. In the limit of extremely asymmetric dissipation, lower and upper bounds on the effi-

ciency are obtained. η_{AB} serves as the upper bound in the former case and lower bound in the later case, thus separating the entire parameter regime of η^E into two parts. To this end, we want to remark that although the two-parameter global maximum of EF does not exist under strong matter-field coupling ($\lambda \gg \Gamma_{h,c}$) and in high temperatures limit, for the general case—where λ may be comparable to $\Gamma_{h,c}$, numerical results indicate that the global maximum of EF may exist (See Fig. 5). But, it is difficult to obtain analytic expressions for EMEF in this case.

Finally, we have compared the performance of a quantum heat engine operating at maximum EF to the engine operating at maximum power. It is inferred that the fractional loss of power is appreciably low in case of engine operating at maximum EF while it produces at least 75% of the power output by the engine working in maximum power regime. These conclusions concur with the optimal performance of a classical endoreversible heat engine operating in the ecological regime [32]. Hence, we conclude that classical as well as quantum heat engines operating at maximum ecological function are much more efficient and environment friendly than the engines operating at maximum power. Therefore, it is reasonable as well as sensible to design real heat engines along the lines of maximizing the ecological function, both for economical and ecological purposes. Similarly, the analogue of ecological function for refrigerators [33, 66] may be employed for quantum models where usually the cooling power is optimized [55, 67].

ACKNOWLEDGEMENTS

V. S. gratefully acknowledges insightful discussions with Professor Robert Alicki. The preliminary results of the above paper were presented at the International conference "Workshop on Quantum and Nano Thermodynamics (WQNT 2018)" held at Alvkärlaby, Sweden, for which financial support provided by Indian Institute of Science Education and Research, Mohali, India, is gratefully acknowledged.

Appendix A: Steady state solution of density matrix equations

Here, we solve the equations for density matrix in the steady state. Substituting the expressions for H_0, \bar{H}, V_0 , and using Eqs. (3) and (4) in Eq. (5), the time evolution of the elements of the density matrix are governed by

following equations:

$$\dot{\rho}_{11} = i\lambda(\rho_{10} - \rho_{01}) - 2\Gamma_h[(n_h + 1)\rho_{11} - n_h\rho_{gg}], \quad (\text{A1})$$

$$\dot{\rho}_{00} = -i\lambda(\rho_{10} - \rho_{01}) - 2\Gamma_c[(n_c + 1)\rho_{00} - n_c\rho_{gg}], \quad (\text{A2})$$

$$\dot{\rho}_{10} = -[\Gamma_h(n_h + 1) + \Gamma_c(n_c + 1)]\rho_{10} + i\lambda(\rho_{11} - \rho_{00}), \quad (\text{A3})$$

$$\rho_{11} = 1 - \rho_{00} - \rho_{gg}, \quad (\text{A4})$$

$$\dot{\rho}_{01} = \dot{\rho}_{10}^*. \quad (\text{A5})$$

$$\rho_{10} = \frac{i\lambda(n_h - n_c)\Gamma_c\Gamma_h}{\lambda^2[(1 + 3n_h)\Gamma_h + (1 + 3n_c)\Gamma_c] + \Gamma_c\Gamma_h[1 + 2n_h + n_c(2 + 3n_h)][(1 + n_c)\Gamma_c + (1 + n_h)\Gamma_h]}, \quad (\text{A6})$$

and

$$\rho_{01} = \rho_{10}^*. \quad (\text{A7})$$

Calculating the trace in Eq. (6), the output power is given by

$$P = i\hbar\lambda(\omega_h - \omega_c)(\rho_{10} - \rho_{01}). \quad (\text{A8})$$

Similarly evaluating the trace in Eq. (7), heat flux \dot{Q}_h can be written as

$$\dot{Q}_h = -\hbar\omega_h(2\Gamma_h[(n_h + 1)\rho_{11} - n_h\rho_{gg}]). \quad (\text{A9})$$

Using the steady state condition $\dot{\rho}_{11} = 0$ (see Eq. (A1)), Eq. (A9) becomes

$$\dot{Q}_h = -i\hbar\lambda\omega_h(\rho_{10} - \rho_{01}). \quad (\text{A10})$$

Solving Eqs. (A1) - (A5) in the steady state by setting $\dot{\rho}_{mn} = 0$ ($m, n = 0, 1$), we obtain

Now EF is given by

$$E = 2P - (1 - \tau)\dot{Q}_h. \quad (\text{A11})$$

Using Eqs. (A8) and (A9), we recast Eq. (A11) as follows

$$E = i\hbar\lambda(\rho_{01} - \rho_{10})[2(\omega_h - \omega_c) - (1 - \tau)\omega_h]. \quad (\text{A12})$$

Substituting Eqs. (A6) and (A7) in Eqs. (A8) and (A12), we have

$$P = \frac{2\hbar\lambda^2\Gamma_c\Gamma_h(n_h - n_c)(\omega_h - \omega_c)}{\lambda^2[(1 + 3n_h)\Gamma_h + (1 + 3n_c)\Gamma_c] + \Gamma_c\Gamma_h[1 + 2n_h + n_c(2 + 3n_h)][(1 + n_c)\Gamma_c + (1 + n_h)\Gamma_h]}, \quad (\text{A13})$$

$$E = \frac{2\hbar\lambda^2\Gamma_c\Gamma_h(n_h - n_c)[2(\omega_h - \omega_c) - \eta_c\omega_h]}{\lambda^2[(1 + 3n_h)\Gamma_h + (1 + 3n_c)\Gamma_c] + \Gamma_c\Gamma_h[1 + 2n_h + n_c(2 + 3n_h)][(1 + n_c)\Gamma_c + (1 + n_h)\Gamma_h]}. \quad (\text{A14})$$

Appendix B: Optimization in the high temperatures limit

In order to obtain analytic expressions of interest, we optimize power output and the EF given above, in the high temperatures limit, while assuming a strong matter-field coupling $\lambda \gg \Gamma_{h,c}$. In the said limit, n_h and n_c can be approximated as

$$n_h = \frac{1}{e^{\hbar\omega_h/k_B T_h} - 1} \simeq \frac{k_B T_h}{\hbar\omega_h}, \quad (\text{B1})$$

$$n_c = \frac{1}{e^{\hbar\omega_c/k_B T_c} - 1} \simeq \frac{k_B T_c}{\hbar\omega_c}. \quad (\text{B2})$$

Using Eqs. (B1) and (B2) in Eq. (A14), and ignoring the terms containing $\Gamma_{h,c}$ in comparison to λ , we can write P and E in terms of $\tau = T_c/T_h$ and $\gamma = \Gamma_h/\Gamma_c$ in the following form

$$P \simeq \frac{2\hbar\Gamma_h(\omega_h - \omega_c)(\omega_c - \tau\omega_h)}{3(\omega_c\gamma + \tau\omega_h)}, \quad (\text{B3})$$

$$E \simeq \frac{2\hbar\Gamma_h(\omega_c - \tau\omega_h)[2(\omega_h - \omega_c) - (1 - \tau)\omega_h]}{3(\omega_c\gamma + \tau\omega_h)}. \quad (\text{B4})$$

One parameter optimization of ecological function

We optimize E w.r.t to either ω_c or ω_h , while keeping the other fixed. Optimizing Eq. (A14) w.r.t ω_c , for a fixed ω_h , and solving for ω_c , we obtain

$$\omega_c^* = \frac{\omega_h}{2\gamma} \left(\sqrt{2\tau(1+\gamma)[\gamma + (2+\gamma)\tau]} - 2\tau \right). \quad (\text{B5})$$

Using Eq. (B5) in Eq. (11), EMEF is given by Eq. (16). Optimizing Eq. (B4) w.r.t ω_h , we have

$$\omega_h^* = \omega_c \frac{\sqrt{(1+\gamma)(1+\tau)[\gamma + 2(1+\gamma)\tau]} - \gamma(1+\tau)}{\tau(1+\tau)}. \quad (\text{B6})$$

In this case, EMEF is given by Eq. (18).

Appendix C: Ratio E/P for two different target functions

Here, we derive the expressions for the ratio E/P for the following four cases.

Optimal E for a fixed ω_h

The optimal value of the EF, $E_{\text{eco}}^{*(\omega_h)}$, can be evaluated by substituting Eq. (B5) into Eq. (B4). Similarly,

$$P_{\text{eco}}^{*(\omega_c)} = \frac{2\hbar\omega_c\Gamma_h((1+\gamma)(1+\tau) + B)((\tau+\gamma)(1+\tau) + B)}{3\tau(1+\tau)B}, \quad (\text{C6})$$

where $B = \sqrt{(1+\gamma)(1+\tau)[\gamma + (2+\gamma)\tau]}$. We evaluate the ratio of $E_{\text{eco}}^{*(\omega_c)}$ and $P_{\text{eco}}^{*(\omega_c)}$ as follows

$$R_{\text{eco}(\gamma)}^{\omega_c} = \frac{B}{(1+\gamma)\tau + B}. \quad (\text{C7})$$

Again the limiting cases $\gamma \rightarrow 0$ and $\gamma \rightarrow \infty$ yield the following two equations

$$R_{\text{eco}(0)}^{\omega_c} = \frac{\sqrt{2(1+\tau)}}{\sqrt{\tau} + \sqrt{2(1+\tau)}}, \quad R_{\text{eco}(\infty)}^{\omega_c} = \frac{1+\tau}{1+2\tau}. \quad (\text{C8})$$

Optimal power with a fixed ω_h

The optimization of power w.r.t ω_c (ω_h fixed) or ω_h (ω_c fixed) is performed in the Ref. [29]. For the former case, the expression for ω_c^{P*} is given by

$$\omega_c^{P*} = \gamma^{-1}[\tau + \sqrt{\tau(1+\gamma)(\tau+\gamma)}]\omega_h. \quad (\text{C9})$$

substituting Eq. (B5) into Eq. (B3), we obtain the expression for power at maximum EF, $P_{\text{eco}}^{*(\omega_h)}$. Therefore, we have

$$E_{\text{eco}}^{*(\omega_h)} = \frac{2\hbar\omega_h\Gamma_h}{3\gamma^2}(\gamma + 4\tau + 3\gamma\tau - 2A), \quad (\text{C1})$$

$$P_{\text{eco}}^{*(\omega_h)} = \frac{\hbar\omega_h\Gamma_h}{3\gamma^2A}(A - 2(\gamma + \tau))(A - 2(1 + \gamma)\tau), \quad (\text{C2})$$

where $A = \sqrt{2(1+\gamma)\tau[\gamma + (2+\gamma)\tau]}$. The ratio of $E_{\text{eco}}^{*(\omega_h)}$ and $P_{\text{eco}}^{*(\omega_h)}$ is evaluated to be

$$R_{\text{eco}(\gamma)}^{\omega_h} = \frac{A}{(1+\gamma)\tau + A}. \quad (\text{C3})$$

Now, consider $\gamma \rightarrow 0$ and $\gamma \rightarrow \infty$. For these limiting cases, the above equation reduces to:

$$R_{\text{eco}(0)}^{\omega_h} = \frac{2}{3}, \quad R_{\text{eco}(\infty)}^{\omega_h} = \frac{\sqrt{2(1+\tau)}}{\sqrt{\tau} + \sqrt{2(1+\tau)}}. \quad (\text{C4})$$

Optimal E for a fixed ω_c

In this case, the expression for optimal EF and the corresponding power output can be obtained by using Eqs. (B6) and (B4), and Eqs. (B6) and (B3), respectively.

$$E_{\text{eco}}^{*(\omega_c)} = \frac{2\hbar\omega_c\Gamma_h(1 + 3\tau + 2\gamma(1 + \tau) - 2B)}{3\tau}, \quad (\text{C5})$$

Again, the expressions for optimal power and for the EF at optimal power are evaluated to be

$$P_{\text{pow}}^{*(\omega_h)} = \frac{2\hbar\omega_h\Gamma_h(\gamma + 2\tau + \gamma\tau - 2C)}{3\gamma^2}, \quad (\text{C10})$$

$$E_{\text{pow}}^{*(\omega_h)} = \frac{2\hbar\omega_h\Gamma_h(C - (1 + \gamma)\tau)(C - 2\tau - (1 + \tau)\gamma)}{\gamma^2C}, \quad (\text{C11})$$

where $C = \sqrt{\tau(1+\gamma)(\tau+\gamma)}$. The required ratio is calculated to be

$$R_{\text{pow}(\gamma)}^{\omega_h} = 1 - \frac{C}{\tau + \gamma}, \quad (\text{C12})$$

from which we can write

$$R_{\text{pow}(0)}^{\omega_h} = 0, \quad R_{\text{pow}(\infty)}^{\omega_h} = 1 - \sqrt{\tau}. \quad (\text{C13})$$

Optimal power with a fixed ω_c

For this case, the optimal value of $\omega_h^{P^*}$ is given by [29]

$$\omega_h^{P^*} = \tau^{-1}[-\gamma + \sqrt{(1+\gamma)(\tau+\gamma)}]\omega_c. \quad (\text{C14})$$

Then, we can obtain

$$P_{\text{pow}}^{*(\omega_c)} = \frac{2\hbar\omega_c\Gamma_h(1+\tau+2\gamma-2D)}{3\tau}, \quad (\text{C15})$$

$$E_{\text{pow}}^{*(\omega_c)} = \frac{(D-(1+\gamma))((1+\tau)D-2\tau-\gamma(1+\tau))}{(2\hbar\omega_c\Gamma_h)^{-1}3\tau\sqrt{(1+\gamma)(\tau+\gamma)}}, \quad (\text{C16})$$

where $D = \sqrt{(1+\gamma)(\tau+\gamma)}$. The ratio of $E_{\text{pow}}^{*(\omega_c)}$ to $P_{\text{pow}}^{*(\omega_c)}$ is evaluated to be

$$R_{\text{pow}(\gamma)}^{\omega_c} = 1 - \frac{(1+\gamma)\tau}{D}, \quad (\text{C17})$$

whose limiting values for $\gamma \rightarrow 0$ and $\gamma \rightarrow \infty$, are

$$R_{\text{pow}(0)}^{\omega_c} = 1 - \sqrt{\tau}, \quad R_{\text{pow}(\infty)}^{\omega_c} = 1 - \tau. \quad (\text{C18})$$

-
- [1] S. Vinjanampathy and J. Anders, *Contemp. Phys.* **57**, 545 (2016).
- [2] J. Millen and A. Xuereb, *New J. Phys.* **18**, 011002 (2016).
- [3] R. Kosloff, *Entropy* **15**, 2100 (2013).
- [4] M. O. Scully, *Phys. Rev. Lett.* **87**, 220601 (2001).
- [5] T. D. Kieu, *Phys. Rev. Lett.* **93**, 140403 (2004).
- [6] H. T. Quan, Y.-x. Liu, C. P. Sun, and F. Nori, *Phys. Rev. E* **76**, 031105 (2007).
- [7] A. E. Allahverdyan, R. S. Johal, and G. Mahler, *Phys. Rev. E* **77**, 041118 (2008).
- [8] G. Thomas and R. S. Johal, *Phys. Rev. E* **83**, 031135 (2011).
- [9] S. Abe, *Phys. Rev. E* **83**, 041117 (2011).
- [10] G. S. Agarwal and S. Chaturvedi, *Phys. Rev. E* **88**, 012130 (2013).
- [11] A. del Campo, J. Goold, and M. Paternostro, *Sci. Rep.* **4**, 6208 (2014).
- [12] F. Altintas, A. U. C. Hardal, and O. E. Müstecaplıođlu, *Phys. Rev. E* **90**, 032102 (2014).
- [13] A. Insinga, B. Andresen, and P. Salamon, *Phys. Rev. E* **94**, 012119 (2016).
- [14] S. Chand and A. Biswas, *Phys. Rev. E* **95**, 032111 (2017).
- [15] V. Mehta and R. S. Johal, *Phys. Rev. E* **96**, 032110 (2017).
- [16] B. K. Agarwalla, J.-H. Jiang, and D. Segal, *Phys. Rev. B* **96**, 104304 (2017).
- [17] G. Thomas, N. Siddharth, S. Banerjee, and S. Ghosh, *Phys. Rev. E* **97**, 062108 (2018).
- [18] F. L. Curzon and B. Ahlborn, *Am. J. Phys.* **43**, 22 (1975).
- [19] M. Esposito, R. Kawai, K. Lindenberg, and C. Van den Broeck, *Phys. Rev. Lett.* **105**, 150603 (2010).
- [20] Y. Izumida and K. Okuda, *Europhys. Lett.* **97**, 10004 (2012).
- [21] M. Esposito, R. Kawai, K. Lindenberg, and C. Van den Broeck, *Phys. Rev. E* **81**, 041106 (2010).
- [22] O. Abah, J. Roßnagel, G. Jacob, S. Deffner, F. Schmidt-Kaler, K. Singer, and E. Lutz, *Phys. Rev. Lett.* **109**, 203006 (2012).
- [23] R. Wang, J. Wang, J. He, and Y. Ma, *Phys. Rev. E* **87**, 042119 (2013).
- [24] J. Jaramillo, M. Beau, and A. del Campo, *New J. Phys.* **18**, 075019 (2016).
- [25] M. Campisi and R. Fazio, *Nat. Comm.* **7**, 11895 (2016).
- [26] G. Watanabe, B. P. Venkatesh, P. Talkner, and A. del Campo, *Phys. Rev. Lett.* **118**, 050601 (2017).
- [27] P. A. Erdman, F. Mazza, R. Bosisio, G. Benenti, R. Fazio, and F. Taddei, *Phys. Rev. B* **95**, 245432 (2017).
- [28] V. Cavina, A. Mari, and V. Giovannetti, *Phys. Rev. Lett.* **119**, 050601 (2017).
- [29] K. E. Dorfman, D. Xu, and J. Cao, *Phys. Rev. E* **97**, 042120 (2018).
- [30] J. Chen, Z. Yan, G. Lin, and B. Andresen, *Energy Convers. and Manage.* **42**, 173 (2001).
- [31] A. de Vos, *Endoreversible Thermodynamics of Solar Energy Conversion* (Oxford University Press, Oxford, UK, 1992).
- [32] F. Angulo-Brown, *J. Appl. Phys.* **69**, 7465 (1991).
- [33] V. Singh and R. S. Johal, *Entropy* **19**, 576 (2017).
- [34] A. C. Hernández, A. Medina, J. M. M. Roco, J. A. White, and S. Velasco, *Phys. Rev. E* **63**, 037102 (2001).
- [35] T. Yilmaz, *J. Energy Inst.* **79**, 38 (2006).
- [36] V. Singh and R. S. Johal, *Phys. Rev. E* **98**, 062132 (2018).
- [37] H. E. D. Scovil and E. O. Schulz-DuBois, *Phys. Rev. Lett.* **2**, 262 (1959).
- [38] A. U. C. Hardal and O. E. Müstecaplıođlu, *Sci. Rep.* **5**, 12953 (2016).
- [39] D. Türkençe and O. E. Müstecaplıođlu, *Phys. Rev. E* **93**, 012145 (2016).
- [40] M. O. Scully, K. R. Chapin, K. E. Dorfman, M. B. Kim, and A. Svidzinsky, *Proc. Natl. Acad. Sci. USA* **108**, 15097 (2011).
- [41] H. P. Goswami and U. Harbola, *Phys. Rev. A* **88**, 013842 (2013).
- [42] C. L. Latune, I. Sinayskiy, and F. Petruccione, *Quantum Science and Technology* **4**, 025005 (2019).
- [43] R. Uzdin, A. Levy, and R. Kosloff, *Phys. Rev. X* **5**, 031044 (2015).

- [44] T. Zhang, W.-T. Liu, P.-X. Chen, and C.-Z. Li, *Phys. Rev. A* **75**, 062102 (2007).
- [45] G. F. Zhang, *Phys. Rev. A* **49**, 123 (2008).
- [46] H. Wang, S. Liu, and J. He, *Phys. Rev. E* **79**, 041113 (2009).
- [47] K. V. Hovhannisyán, M. Perarnau-Llobet, M. Huber, and A. Acín, *Phys. Rev. Lett.* **111**, 240401 (2013).
- [48] A. Hewgill, A. Ferraro, and G. De Chiara, *Phys. Rev. A* **98**, 042102 (2018).
- [49] X. L. Huang, T. Wang, and X. X. Yi, *Phys. Rev. E* **86**, 051105 (2012).
- [50] J. Roßnagel, O. Abah, F. Schmidt-Kaler, K. Singer, and E. Lutz, *Phys. Rev. Lett.* **112**, 030602 (2014).
- [51] R. Alicki and D. Gelbwaser-Klimovsky, *New J. Phys.* **17**, 115012 (2015).
- [52] E. Geva and R. Kosloff, *J. Chem. Phys.* **97**, 4398 (1992).
- [53] E. Geva and R. Kosloff, *J. Chem. Phys.* **96**, 3054 (1992).
- [54] L. A. Correa, J. P. Palao, D. Alonso, and G. Adesso, *Sci. Rep* **4**, 3949 (2014).
- [55] L. A. Correa, J. P. Palao, G. Adesso, and D. Alonso, *Phys. Rev. E* **90**, 062124 (2014).
- [56] M. Kilgour and D. Segal, *Phys. Rev. E* **98**, 012117 (2018).
- [57] S. Nimmrichter, J. Dai, A. Roulet, and V. Scarani, *Quantum* **1**, 37 (2017).
- [58] E. Geva and R. Kosloff, *Phys. Rev. E* **49**, 3903 (1994).
- [59] E. Geva and R. Kosloff, *J. Chem. Phys.* **104**, 7681 (1996).
- [60] E. Boukobza and D. J. Tannor, *Phys. Rev. A* **74**, 063823 (2006).
- [61] E. Boukobza and D. J. Tannor, *Phys. Rev. A* **74**, 063822 (2006).
- [62] E. Boukobza and D. J. Tannor, *Phys. Rev. Lett.* **98**, 240601 (2007).
- [63] R. Alicki, *J. Phys. A* **12**, L103 (1979).
- [64] C. de Tomás, J. M. M. Roco, A. C. Hernández, Y. Wang, and Z. C. Tu, *Phys. Rev. E* **87**, 012105 (2013).
- [65] R. Long, Z. Liu, and W. Liu, *Phys. Rev. E* **89**, 062119 (2014).
- [66] Z. Yan and L. Chen, *Journal of Physics D: Applied Physics* **29**, 3017 (1996).
- [67] P. A. Erdman, B. Bhandari, R. Fazio, J. P. Pekola, and F. Taddei, *Phys. Rev. B* **98**, 045433 (2018).